

AD-A064 364

AIR FORCE INST OF TECH WRIGHT-PATTERSON AFB OHIO SCH--ETC F/G 15/4
PERFORMANCE IMPROVEMENT OF A CLASS OF ARRAY PROCESSORS IN A JAM--ETC(U)
DEC 78 R E LESHER

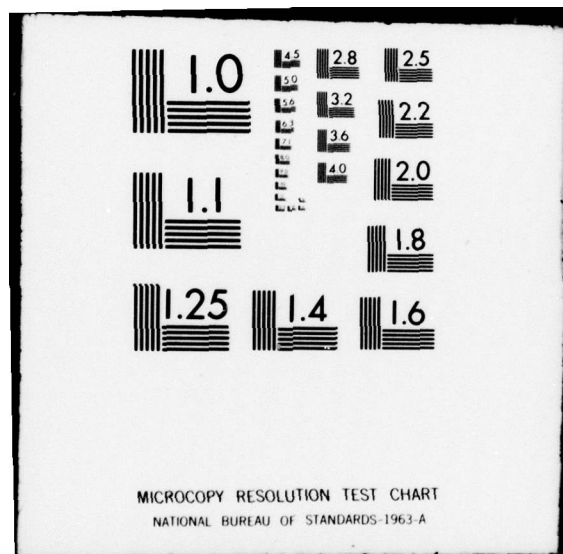
UNCLASSIFIED

AFIT/6E/EE/78-33

NL

| OF |
AD
A064364

END
DATE
FILMED
4-79
DDC



MICROCOPY RESOLUTION TEST CHART
NATIONAL BUREAU OF STANDARDS-1963-A

AFIT/GE/EE/78-33

①
LEVEL *gt*

ADA 064364

DDC FILE COPY

PERFORMANCE IMPROVEMENT OF A CLASS
OF ARRAY PROCESSORS IN A JAMMING
ENVIRONMENT

THESIS

AFIT/GE/EE/78-33

Ronnie E. Leshner
Capt USAF

Approved for public release; distribution unlimited

DDC
RECEIVED
FEB 9 1979
A

79 01 30 142

14

AFIT/GE/EE/78-33

6

PERFORMANCE IMPROVEMENT OF A CLASS OF ARRAY PROCESSORS IN A JAMMING ENVIRONMENT.

9

Master's THESIS

16

2277

Presented to the Faculty of the School of Engineering of the Air Force Institute of Technology Air Training Command in Partial Fulfillment of the Requirements for the Degree of Master of Science Electrical Engineering

12) 64p

ACCESSION FOR	
DTIC	White Section <input checked="" type="checkbox"/>
DDP	Self Section <input type="checkbox"/>
CLASSIFIED	<input type="checkbox"/>
JUSTIFICATION	
BY	
DISTRIBUTION AVAILABILITY CODE	
REF. STATE OF ORIGIN	
A	

10

Ellis Ronnie N. / Leshner B.S., M.S.S.M.

Captain USAF

Graduate Electrical Engineering

11

Dec 78

Approved for public release; distribution unlimited.

012 225

Jim

Acknowledgements

The author would like to extend his sincere appreciation to his thesis advisor and thesis committee chairman, Captain Stanley R. Robinson, for the guidance he provided in the completion of this thesis. His insight and understanding of the many peripheral areas related to the thesis topic greatly aided the author in maintaining a singular and logical approach to the thesis problem. Captain Robinson formally introduced the author to the theory of signal detection and estimation which formed the basis of this thesis.

The author gratefully acknowledges the support of his typist, Mrs. Dorothy Williams. Her patience during the draft, revision, and final phases of the thesis permitted the author to concentrate on the writing (and rewriting) of the thesis.

Last, but certainly not least, the author humbly acknowledges the love, understanding, and endurance of his wife, Nancy. It was her unenviable task to live with the author during his two and one-half years as an AFIT student in two academic programs which are culminated by this thesis.

Ronnie E. Leshner

Contents

	Page
Acknowledgements	ii
List of Figures	iv
Abstract	v
I. Introduction	1
II. Statistical Representation of Jamming Signals	5
A. Scalar Field Theory	5
B. Fields as Random Processes	8
C. Second Moment Description of Jammer Fields	9
D. Series Representation of Jammers	16
III. Signal Detection Theory	20
A. Review of Signal Detection Theory	20
B. Optimum Array Processor	23
C. Conventional Array Processor	28
IV. Performance Improvement	31
A. Performance Measure	31
B. N Nearly Orthogonal Jammers	33
C. N Non-Resolvable Jammers	42
D. Signal Jammer, Single Spatial Dimension	44
V. Conclusions and Recommendations	48
A. Conclusions	48
B. Recommendations	50
Bibliography	51
Vita	53

List of Figures

<u>Figure</u>		<u>Page</u>
1	Point Source Propagating to Array Surface	7
2	Point Sources in Far Field of array Representing Jammers and Desired Signal	10
3	Single Plane Wave Arriving at the Array	13
4	Complex Optimum Receiver Configuration	22
5	Optimum Processor for CW Signals and CW Jammers	25
6	Performance Measure, μ , vs s'^2 for 2 Jammers . . .	38
7	Performance Measure, μ , vs s'^2 for 1 Jammer . . .	41
8	Angular Difference ($\theta_s - \theta_n$) vs s^2 ; μ vs q^2 for $\lambda_n = \lambda_s = 0.5\text{m}$, $L = 1\text{m}$, $\frac{J_o \alpha L}{N_o} = 30\text{dB}$	46

Abstract

The purpose of this research is to determine the fundamental performance improvement of an optimum array detector versus a conventional beamformer detector in a jamming environment. The fundamental performance improvement is based on total knowledge of both the desired signal and the jammers, and their respective locations in space. The jammers are modeled as a colored noise component in the binary hypothesis detection problem. Mathematical tractability is achieved by considering distributed measurements in space and time across the array. Conditions are identified which allow determination of the necessary eigenvalues and eigenfunctions by inspection of the propagation functions of plane wave jammers.

Performance improvement is given for several jamming scenarios: two mutually orthogonal jammers, single jammer (two spatial dimensions), band limited jammer, and single jammer (one spatial dimension). The optimum detector performs respectively 68dB, 60dB, 19.5dB, and 20dB better than the beamformer for the jamming scenarios addressed and similar parameters for each case. The maximum performance improvement for the two mutually orthogonal jammers occurs when twenty-five percent of the signal power projects in the direction of each jammer. Maximum improvement for a single jammer occurs when fifty percent of the signal power projects in the direction of the jammer. Performance improvement in

the presence of a spatially bandlimited jammer is due primarily to the degradation of the beamformer's performance. For the scenarios examined, the optimum detector provides significant performance improvement over the conventional beamformer detector.

PERFORMANCE IMPROVEMENT OF A CLASS
OF ARRAY PROCESSORS IN A JAMMING ENVIRONMENT

I. Introduction

Recently much research has been devoted to the subject of multiple sensor or array type antenna systems. This interest has been generated by the ability of the adaptive array antenna systems to provide rapid inertialess scanning for high speed angular coverage, their large power handling capability, and their usability in environments where actual movement of the antenna is difficult or impossible (Gallop, 1971: 2). When using an array system (or any other antenna system), the goal is to process the measurement provided by the array to extract information contained in the received signal as accurately as possible. Heretofore, the design of a radio frequency (RF) communications receiving system has been divided into two segments: the antenna system and the communications processor. Typically, each of these segments was designed and optimized separately. These two optimally designed segments were then united to form a single system which, due to the ad hoc nature of this design approach, may have resulted in an overall sub-optimal receiver processor.

Such a design approach has been motivated by several factors. First, the disciplines of antenna design and processor design were treated as separate and quite distinct areas of academic interest and application. Second, the optimum processor has sometimes led to computations which were unrealizable

from a hardware point of view. This limitation has been somewhat overcome recently by technology with the advent of practical applications of digital processing techniques, surface acoustic wave devices, and charge coupled devices (Dudgeon, 1977:98; Melen and Buss, 1977:327-328).

With the ability to design and potentially build optimum receiver systems at hand, the increased performance gained from the optimum system needs to be compared with the performance of the conventionally designed system. This comparison then becomes a useful tool in assessing the cost relationships related to the two design approaches.

Depending upon the type of signal to be detected by the antenna array processor system, different criteria exist for the performance comparison of the optimum and conventional array systems. For the case of a deterministic signal, the comparison of the output signal to noise ratios (SNR) of each system results in a useful measurement of performance improvement of the optimum antenna array processor over the conventionally designed system (Van Trees, 1968:99). This ratio of SNR is the method adopted to evaluate the fundamental performance improvement of the optimum array processor in this thesis.

Some work has been done in the area of determining the performance of optimum adaptive array receivers. Gallop and Nolte addressed the performance of an array receiver for a signal of unknown spatial location in spatially uncorrelated Gaussian noise. They demonstrated a trade-off among array

parameters and signal parameters relevant to the performance of the detector (Gallop and Nolte, 1974:429-435). In his dissertation, Gallop concluded that he was unable to calculate performance analytically even from the closed form expression for discrete sampling by a two or three sensor array for a signal at an unknown location (Gallop, 1971:73). Adams and Nolte studied the performance of the array for a signal of known location but an uncertain waveform in the presence of spatially uncorrelated noise. They found that the detection performance was equal to the performance of the scalar processor with input signal to noise ratio increased by a scalar factor (Adams and Nolte, 1975:656-669). Hodgkiss and Nolte addressed the performance degradation for the array processor when uncertainty exists in the direction of the signal, noise source, or both (Hodgkiss and Nolte, 1976:605-615). All of the performance results obtained by the previous studies included the effects of unknown signal properties (direction, power, etc.) as well as uncertainty in the noise source properties. The inclusion of these uncertain properties clouds the issue of fundamentally how much better the optimum array receiver does perform over any other array receiver in the presence of jamming.

Pasupathy developed a performance comparison between an optimum and conventional array processor using a distributed (spatially continuous) measurement to simplify the mathematics associated with a discrete element array. His work, however, addressed only one spatial dimension and one noise model for a passive sonar signal problem and did not

include the effects of signal or noise uncertainty (Pasupathy, 1978:158-164).

Examination of the fundamental performance improvement of an optimum array processor in the presence of spatially correlated noise (jammers) is the central issue of this thesis. The approach to be followed extends Pasupathy's work to two spatial dimensions and examines several different jamming environments. The performance of the optimum processor is considered a benchmark since the signal of interest is assumed to be fully known and thus represents the most improvement which the optimum array processor can provide in the jamming environment.

The following chapters will address the representation of the jamming signals as spatially colored noise. A review of detection theory will be followed by the performance improvement results of the optimum array processor. Conclusions drawn from these results and any recommendation for additional research will be presented in the final chapter.

II. Statistical Representation of Jamming Signals

This chapter addresses four topics in developing the statistical representation of jamming signals. These topics are: (1) scalar field theory, (2) fields as random processes, (3) second moment description of jammer fields, and (4) series representation of jammers.

A. Scalar Field Theory

Before looking at any representation of a jamming signal it is necessary to establish a notation convention which is based on scalar field theory. Consider first the scalar field given by:

$$u(t,x,y,z) = A(t,x,y,z)\cos[2\pi f_0 t - \phi(t,x,y,z)] \quad (1)$$

which is a function of both time and space coordinates. This expression can more easily be written as:

$$u(t,x,y,z) = \text{Re}\{U(t,x,y,z)\exp[-j2\pi f_0 t]\} \quad (2)$$

where

$$U(t,x,y,z) = A(t,x,y,z)\exp[j\phi(t,x,y,z)] \quad (3)$$

$U(t,x,y,z)$ is called the complex envelope of the scalar field. This representation is appropriate for both electric and magnetic fields. For the purpose at hand, the representation is of an electric field with units of volts/meter/ $\sqrt{\text{ohm}}$. It is easy to see that the complex envelope contains all the information of the field centered at f_0 .

Scalar field theory and the use of the complex envelope

permit a straightforward means of representing a signal impinging on an array surface. Fig. 1 shows the signal originating from a point source, propagating through space and striking the array surface. When the distance between the array surface and the point source is large enough then the wavefront striking the array surface is a plane wave (Gagliardi and Karp, 1967:13). For ease of notation it is convenient to consider the field at a specific value of the z coordinate, thus reducing the complex envelope representation to two spatial dimensions. With this notation in mind, the complex envelope of the plane wave striking the array is given by:

$$U(t,x,y) = A(t)\exp[j\psi(t)]\exp[j(v_x x + v_y y)] \quad (4)$$

where

$$v_x = \frac{2\pi}{\lambda} \cos\theta$$

and

$$v_y = \frac{2\pi}{\lambda} \cos\phi$$

where λ is the wavelength of the plane wave given by:

$$\lambda = \frac{c}{f_0} \quad (5)$$

where c is the speed of light and f_0 is the frequency of the wave. $A(t)$ is the time varying amplitude of the plane wave and $\psi(t)$ is the time varying phase of the plane wave. When $A(t)$ and $\psi(t)$ are constant for all values of t then the plane

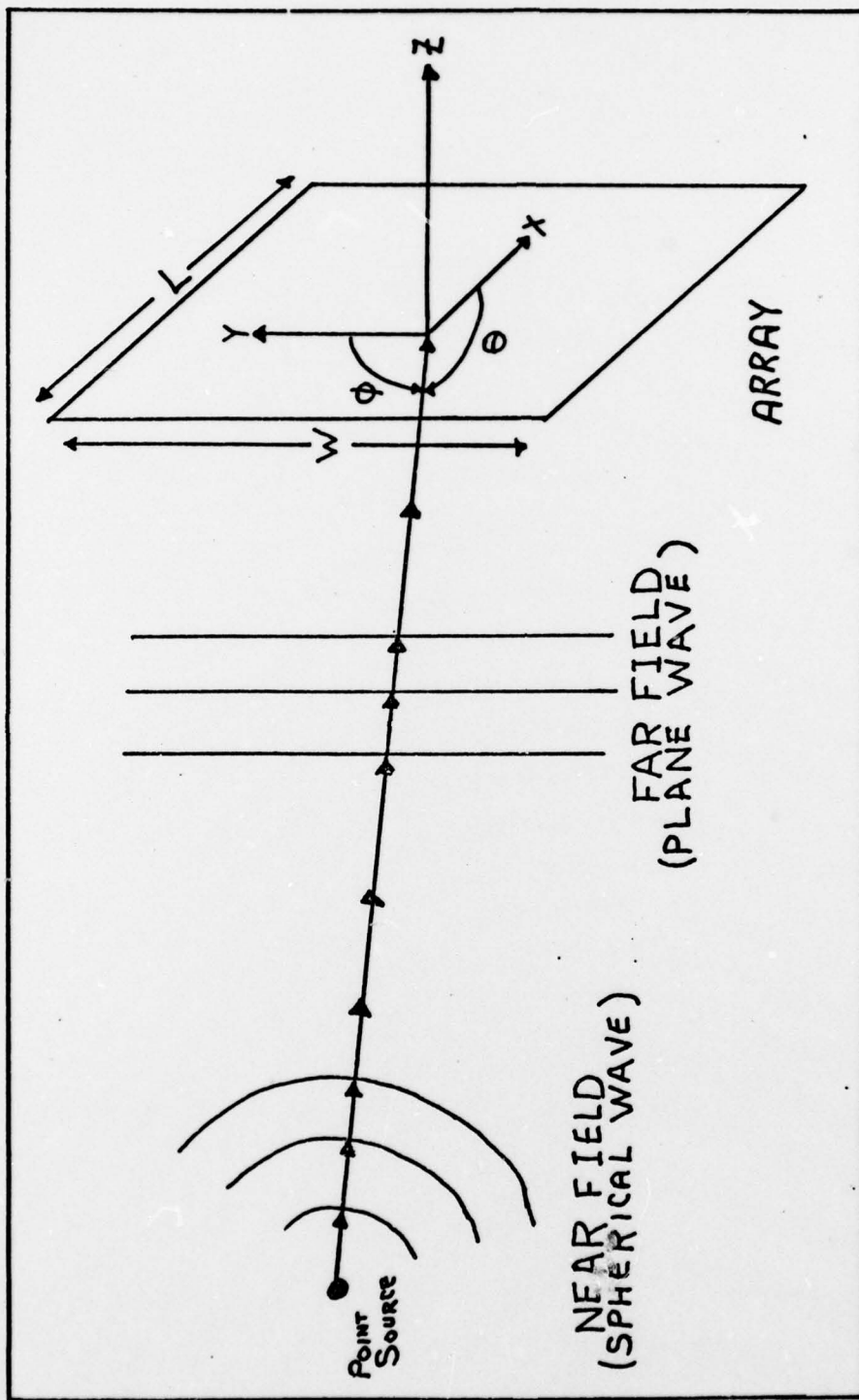


Figure 1. Point source propagating to array surface.

wave is said to be monochromatic. When the bandwidth, B , is much less than the center frequency, f_0 , the plane wave is said to be quasi-monochromatic (Gagliardi and Karp, 1976:13-17). Otherwise the plane wave is non-monochromatic.

B. Fields as Random Processes

When the fields of interest are unknown, it is convenient to model them as complex random processes in time and space. The purpose of this section is to develop a notation for these random processes.

Consider first a complex representation of the field:

$$U(t, \bar{r}) = U_R(t, \bar{r}) + jU_I(t, \bar{r}) \quad (6)$$

where $U_R(t, \bar{r})$ and $U_I(t, \bar{r})$ are the real and imaginary parts of $U(t, \bar{r})$. The notation \bar{r} is the vector representation of the point described by the coordinates x and y .

The first moment of the random field is defined as:

$$\begin{aligned} E[U(t, \bar{r})] &= E[U_R(t, \bar{r})] + jE[U_I(t, \bar{r})] \\ &= M_R(t, \bar{r}) + jM_I(t, \bar{r}) \triangleq M(t, \bar{r}) \end{aligned} \quad (7)$$

Given the first moment of the random field, the second moments can be obtained from the correlation functions, $E[U_R(t, \bar{r})U_R(t', \bar{r}')]$ and $E[U_I(t, \bar{r})U_I(t', \bar{r}')]$, and the cross correlation, $E[U_R(t, \bar{r})U_I(t', \bar{r}')]$. Direct evaluation shows that the same information is contained in the complex terms $E[U(t, \bar{r})U(t', \bar{r}')]$ and $E[U(t, \bar{r})U^*(t', \bar{r}')]$ for complex envelopes.

When working with random fields typical assumptions are that the real and imaginary parts have the same correlation functions and that they are uncorrelated and have zero mean.

Hence,

$$\begin{aligned} E[U(t, \bar{r})U^*(t', \bar{r}')] &= R(t, \bar{r}, t', \bar{r}') \\ &= 2E[U_R(t, \bar{r})U_R^*(t', \bar{r}')] \end{aligned} \quad (8)$$

where $R(t, \bar{r}, t', \bar{r}')$ is the correlation function of the field represented by $U(t, \bar{r})$. Several cases of the correlation function are of interest for later use:

(a) Temporally Stationary:

$$R(t, \bar{r}, t', \bar{r}') = R(\bar{r}, \bar{r}', \tau) \quad (9a)$$

where $\tau = t - t'$

(b) Spatially Stationary:

$$R(t, \bar{r}, t', \bar{r}') = R(\bar{r} - \bar{r}', t, t') \quad (9b)$$

(c) Coherence Separable

$$R(t, \bar{r}, t', \bar{r}') = R_t(t, t') R_s(\bar{r}, \bar{r}') \quad (9c)$$

where $R_t(t, t')$ and $R_s(\bar{r}, \bar{r}')$ are the temporal and spatial correlation functions respectively.

C. Second Moment Description of Jammer Fields

The question of how to model a jamming environment can be considered from a number of aspects depending upon the information available about the jammer. For the case at hand, consider a set of point sources in the far field of the array of which one of the point sources is the signal of interest and the other point sources are jammers as shown in Fig 2. Since the point sources are in the far field, this implies that the wave fronts arriving at the array are nearly plane

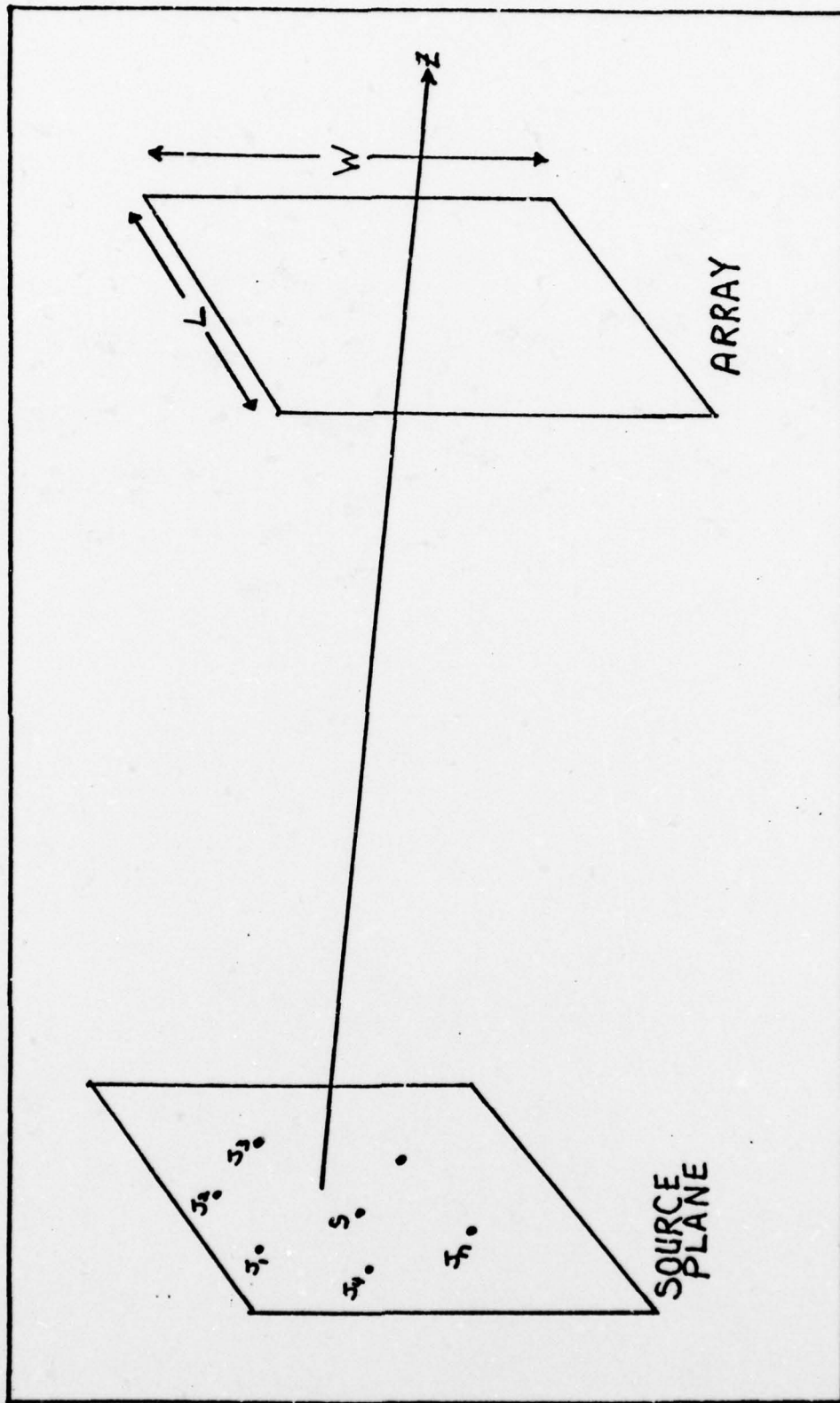


Figure 2. Point sources in far field of array representing jammers and desired signal (s).

waves. The detection problem for the jamming environment becomes one of deciding whether or not the desired signal is present in the plane waves striking the array. In order to solve this detection problem, it is necessary to look at the second moment properties of the jammers.

To account for both jammers and the thermal noise of the array (always present), the total noise interference is considered to be a spatially non-white Gaussian noise composed of an independent white component which is both temporally and spatially stationary representing the thermal noise of the array and a colored component representing the jammer (Van Trees, 1968:287-288). The use of a colored component representation allows for the inclusion of several jammer scenarios without significantly changing the detection problem for the array. Generally, for the array problem, the noise term is given by:

$$n(t, \bar{r}) = w(t, \bar{r}) + n_c(t, \bar{r}) \quad (10)$$

This leads to the following general representation of the noise covariance:

$$K_N(t, t', \bar{r}, \bar{r}') = N_0 \delta(t-t') \delta(\bar{r}-\bar{r}') + K_c(t, t', \bar{r}, \bar{r}') \quad (11)$$

where N_0 is the one-sided spectral density of the white component with units of watt/m²-sec. The use of the white noise component to represent the thermal noise of the array is physically pleasing since the thermal noise is a broad-band noise which is typically independent and identically

distributed from sensor to sensor in the array. Additionally $K_N(t, t', \bar{r}, \bar{r}')$ and $K_C(t, t', \bar{r}, \bar{r}')$ are the covariance functions of the total noise and colored component respectively.

The task now is to form both the total noise and colored covariances. After forming these covariances, an interpretation of the various jamming scenarios and the types of covariances they imply is necessary.

First, as mentioned before, a single jammer is represented as a plane wave emanating from a point source in the far field. The complex envelope representation of the plane wave jammer is

$$J(t, x, y) = \underline{A}(t) \exp[j\underline{\psi}(t)] \exp[j(v_x x + v_y y)] \quad (12)$$

$$\text{where } v_x = \frac{\cos\theta}{\lambda} \quad \text{and } v_y = \frac{\cos\phi}{\lambda}$$

are the spatial frequencies of the plane wave and θ and ϕ are the incident angles measured relative to the array's x and y axes respectively (See Fig 3). Eq (12) can be rewritten as

$$J(t, x, y) = \underline{B}(t) \exp[j(v_x x + v_y y)] \quad (13)$$

$$\text{where } \underline{B}(t) = \underline{A}(t) \exp[j\underline{\psi}(t)]$$

and $\underline{B}(t)$ is a complex random process. If more than one jammer is present, then the total jamming representation, $J_T(t, x, y)$, is:

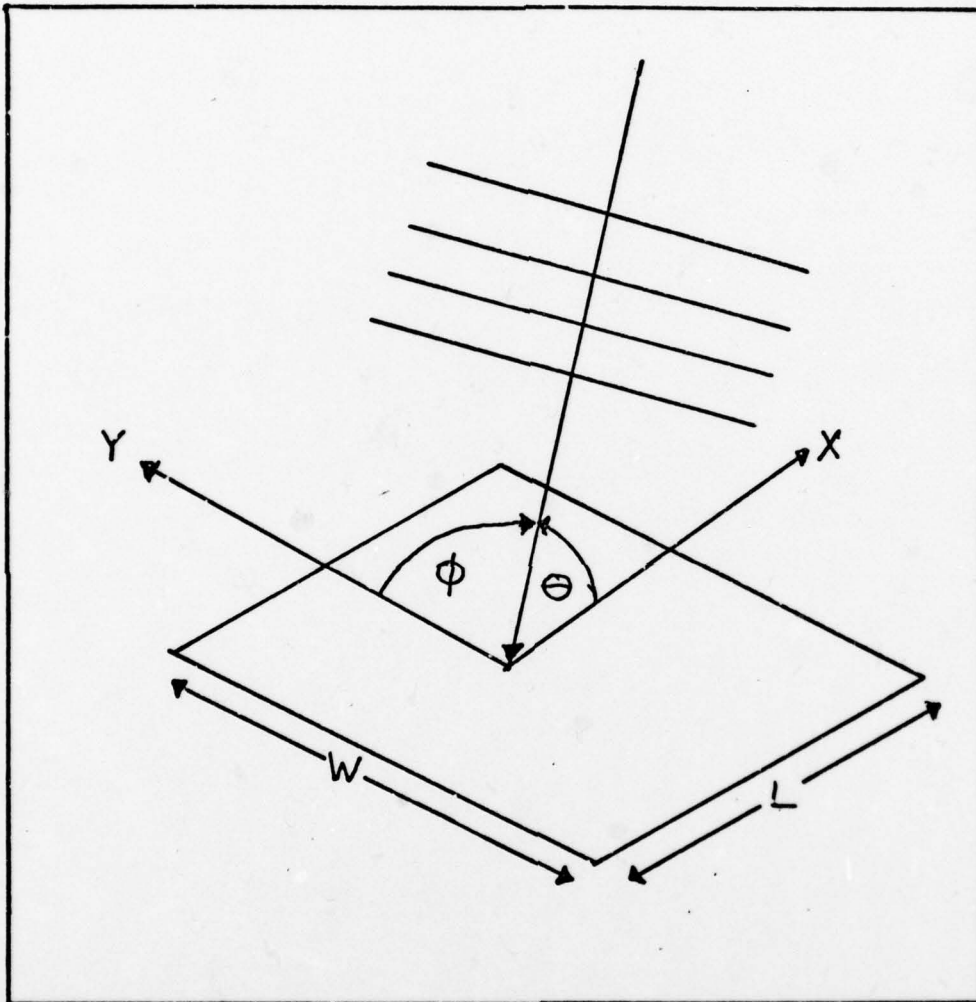


Figure 3. Single plane wave arriving at the array

$$J_T(t, x, y) = \sum_{i=1}^N J_i(t, x, y) = \sum_{i=1}^N B_i(t) \exp[j(v_{xi}x + v_{yi}y)] \quad (14)$$

where N is the number of jammers present and v_{xi} and v_{yi} are the spatial frequencies of each individual jammer. It is assumed that the jammers are uncorrelated, independent and identically distributed. Additionally, the expected value of each individual jammer's complex random amplitude, $B_i(t)$, is zero. This leads to the realization that the covariance function of the colored component is the autocorrelation function. The real and imaginary parts of $J_T(t, x, y)$ have the same correlation functions. It is also assumed that the jammers are temporally stationary (recall Eq (9a)). Hence, the general autocorrelation function for the N jammers is:

$$\begin{aligned} R_c(t, t', x, y, x', y') &= E[J_T(t, x, y) J_T^*(t', x', y')] \\ &= \sum_{i=1}^N R_i(\tau) \exp\{j[v_{ix}(x-x') + v_{iy}(y-y')]\} \end{aligned} \quad (15)$$

where $R_i(\tau)$ is the individual temporally stationary autocorrelation functions of the time varying amplitudes of the jammers. Note that the individual terms in Eq (15) are in the form given by Eq (9c) for temporally and spatially separable autocorrelation functions.

The total noise autocorrelation is

$$R_N(\tau, \bar{r} - \bar{r}') = N_0 \delta(\tau) \delta(\bar{r} - \bar{r}') + \sum_{i=1}^N R_i(\tau) \exp\{j[v_{ix}(x-x') + v_{iy}(y-y')]\} \quad (16)$$

Note that the spatially colored component is also spatially stationary due to the properties of complex exponentials. This representation of the total noise autocorrelation is very difficult to manipulate mathematically in the equations associated with the signal detection problem. Thus, to further reduce this problem, consider representing $R_i(\tau)$ as:

$$R_i(\tau) = \alpha_i R_J(\tau) \quad (17)$$

This says that all of the jammers have the same temporal statistics but may have different average power levels. By redefining the exponential in the colored component as:

$$\exp[j(v_{ix}x + v_{iy}y)] = \phi_i(\bar{r}) \quad (18)$$

and

$$\exp[j(v_{ix}x' + v_{iy}y')] = \phi_i(\bar{r}') \quad (19)$$

then Eq (16) becomes:

$$R_N(\tau, \bar{r} - \bar{r}') = N_0 \delta(\tau) \delta(\bar{r} - \bar{r}') + R_J(\tau) \sum_{i=1}^N \alpha_i \phi_i(\bar{r}) \phi_i^*(\bar{r}') \quad (20)$$

where:

$$R_c(\tau, \bar{r} - \bar{r}') = R_J(\tau) \sum_{i=1}^N \alpha_i \phi_i(\bar{r}) \phi_i^*(\bar{r}') \quad (21)$$

Eq (20) is in the general form given for a separable kernel by Van Trees (Van Trees, 1968:316) if the α_i are the eigenvalues, the $\phi_i(\bar{r})$ are the eigenfunctions, and $R_J(\tau)$ is a constant. If $R_J(\tau)$ is not a constant, the separable kernel is still present for only the spatial part of the correlation functions. To be able to use this interpretation, it is

necessary to develop an intuition about the kernels implied by various jamming scenarios. This intuition is based on a series representation of the jammers.

D. Series Representation of the Jamming Signals

In general the composite jamming signal can be represented as a spatial Fourier series expansion at a fixed time. This expansion is given by:

$$J(x,y) = \sum_{n=-\infty}^{\infty} \tilde{J}_n \exp[j\frac{n2\pi}{L}x + j\frac{n2\pi}{W}y] \quad (22)$$

where the random variable \tilde{J}_n are given by

$$\tilde{J}_n = \frac{1}{LW} \int_{-\frac{L}{2}}^{\frac{L}{2}} \int_{-\frac{W}{2}}^{\frac{W}{2}} J(x,y) \exp[-j\frac{n2\pi}{L}x - j\frac{n2\pi}{W}y] dx dy \quad (23)$$

When the L and W are large enough the \tilde{J}_n are approximately uncorrelated (Papoulis, 1965:456). Having the \tilde{J}_n uncorrelated means that $\exp[j\frac{n2\pi}{L}x + j\frac{n2\pi}{W}y]$ approximates the eigenfunctions of a continuous correlation function (Davenport and Root, 1958:97).

In general, a correlation function $R(\bar{r}, \bar{r}')$ can be represented as a Karhunen-Loéve expansion:

$$R(\bar{r}, \bar{r}') = \sum_{n=1}^{\infty} \beta_1 \zeta_1(\bar{r}) \zeta_1^*(\bar{r}') \quad (24)$$

where the β_1 are the eigenvalues and the $\zeta_1(\bar{r})$ are eigenfunctions of the correlation function and a solution of:

$$\beta_1 \zeta_1(\bar{r}) = \int_{-L/2}^{L/2} \int_{-W/2}^{W/2} R(\bar{r}, \bar{r}') \zeta_j^*(\bar{r}') d\bar{r}' \quad (25)$$

An examination of Eq (24) indicates useful interpretations implied by several jammer scenarios. First, a single jammer or a single jammer which is significantly more powerful than the other jammers approximates the condition when there is a single dominant eigenvalue. When there are multiple jammers which are approximately equal strengthed and weak compared to the thermal noise of the array then all of the eigenvalues are equal and approximately equal to N_0 . The condition of multiple jammers which are of different strengths and resolvable by the array implies that the eigenvalues and eigenfunctions are finite in number.

The last scenario which was described is the same situation (finite number of eigenvalues and eigenfunctions) that Van Trees requires to get his separable kernel for the detection problem. Since it has been shown that the complex exponentials are the eigenfunctions when $(J(x,y))$ is expanded such that the Fourier coefficients are uncorrelated, then the exponentials are also approximately the eigenfunctions for the spatial correlation function of the plane wave jammer. This spatial correlation function is given by the spatial part of Eq (21):

$$R_s(\bar{r}, \bar{r}') = \sum_{i=1}^N \alpha_i \phi_i(\bar{r}) \phi_i^*(\bar{r}') \quad (26)$$

To insure that the $\phi_i(\bar{r})$ are orthogonal the following criterion must be satisfied

$$\delta_{ij} = \text{sinc} \left[\frac{\pi L}{\lambda} (\cos \theta_i - \cos \theta'_j) \right] \text{sinc} \left[\frac{\pi W}{\lambda} (\cos \phi_i - \cos \phi'_j) \right] \quad (27)$$

where θ_i and θ'_j are the angles associated with x and x' respectively, and similarly for ϕ_i and ϕ'_j and y and y' . The term δ_{ij} is the Kronecker delta function. The sinc function is obtained by rewriting the exponentials in Eq (26) using Euler's equation and observing the following definition of the sinc function

$$\text{sinc}(x) = \frac{\sin x}{x} \quad (28)$$

Satisfying Eq (27) yields a finite set of orthogonal functions which must be normalized by $\frac{1}{\sqrt{LW}}$ to get the orthonormal eigenfunctions. (The set of functions obtained visually from the correlation function given by Eq (26) may not be a complete set of eigenfunctions in which case the set of functions from Eq (26) would be an approximation of the set of eigenfunctions.) Thus when the $\phi_i(\bar{r})$ are normalized the resulting correlation function is:

$$R_s(\bar{r}-\bar{r}') = LW \sum_{i=1}^N \alpha_i T_i(\bar{r}) T_i^*(\bar{r}') \quad (29)$$

where $T_i(\bar{r}) = \frac{\phi_i(\bar{r})}{\sqrt{LW}}$ and α_i are the eigenvalues. Eq (29) is

now the proper form for Van Trees's separable kernel. Thus, when the form of the correlation of the N plane waves is given by Eq (26) and the angular locations of the jammers are restricted such that Eq (27) is true, then the eigenfunctions can be identified by inspection and used to develop the separable kernel. When the jammers are not plane wave jammers or they are not mutually orthogonal then the eigenvalues and eigenfunctions must be computationally found by solving Eq (25). The difficulty associated with this computation motivates considering only plane wave jammers who satisfy the criterion of Eq (27) and are thus nearly orthogonal to each other.

From the foregoing discussion, the concept of representing the jammers as a colored noise component of the noise in the signal detection problem has been developed. Assumptions which facilitate the use of this concept have been established in preparation for addressing the signal detection problem and the performance evaluation of the optimum array receiver in the presence of jamming.

III. Signal Detection Theory

This chapter briefly reviews the formalism associated with a binary hypothesis detection problem and then identified the general structure for both the optimum array processor and the conventional array processor. The signal detection review primarily summarizes the results found in Van Trees (Van Trees, 1968:287-333) for a signal with single temporal and two spatial dimensions in the presence of spatially non-white gaussian noise.

A. Review of Signal Detection Theory

The binary hypothesis problem requires the processor to decide which of two hypothesis has occurred based upon the received wave form. The problem is expressed as:

$$\begin{aligned} H_1: r(t,x,y) &= s(t,x,y) + n(t,x,y) \quad t \in [0,T], x \in [-\frac{L}{2}, \frac{L}{2}], y \in [-\frac{W}{2}, \frac{W}{2}] \\ H_0: r(t,x,y) &= n(t,x,y) \end{aligned} \quad (30)$$

where $r(t,x,y)$ is the complex received signal, $s(t,x,y)$ is the known signal, and $n(t,x,y)$ is the spatially non-white gaussian noise. The noise term consists of white and colored components to represent the presence of thermal noise and jamming signals as previously discussed. The signal energy is given by:

$$E = \int_0^T \int_{-\frac{L}{2}}^{\frac{L}{2}} \int_{-\frac{W}{2}}^{\frac{W}{2}} s(t,x,y) s^*(t,x,y) dt dx dy \quad (31)$$

where the array is L by W and the observation interval is $[0,T]$.

The optimum processor computes the likelihood ratio or, if the likelihood ratio is reducible, the sufficient statistic. For the purpose at hand, the sufficient statistic, $\ell(r)$, is given by:

$$\ell(r) = \int_0^T \int_{-\frac{L}{2}}^{\frac{L}{2}} \int_{-\frac{W}{2}}^{\frac{W}{2}} r(t,x,y) g^*(t,x,y) dt dx dy \quad (32)$$

where $g(t,x,y)$ is called the Fredholm resolvent and is the solution of the integral equation:

$$s(t,\bar{r}) = \int_0^T \int_{-\frac{L}{2}}^{\frac{L}{2}} \int_{-\frac{W}{2}}^{\frac{W}{2}} g(t',\bar{r}') R_N(\tau, \bar{r}-\bar{r}') dt' d\bar{r}' \quad (33)$$

where $R_N(\tau, \bar{r}-\bar{r}')$ is the autocorrelation function of the noise. Fig. 4 illustrates the processor.

Of course, once the optimum processor is developed, the issue of interest is measuring the performance of the optimum processor. This measure is obtained by calculating the probability of a decision error for the processor. The probability of error for a binary hypothesis problem, where the hypotheses are equally likely, is:

$$P(\text{error}) = \text{erfc}\left(\frac{d}{2}\right) \quad (34)$$

and

$$\text{erfc}(x) \triangleq \int_x^\infty \frac{1}{\sqrt{2\pi}} \exp\left[-\frac{x^2}{2}\right] dx \quad (35)$$

where d is the geometric distance between the means of the densities scaled by the standard deviation and given by (Van Trees, 1968:99):

$$d^2 \triangleq \frac{[E(\ell|H_1) - E(\ell|H_0)]^2}{\text{Var}(\ell|H_0)} \quad (36)$$

Since the $\text{erfc}(x)$ is a monotonic function, a comparison of different receivers need only involve the parameter d^2 (Van Trees, 1968:37-38). The parameter d^2 is interpreted as the output signal to noise ratio of the optimum detector (Adams,

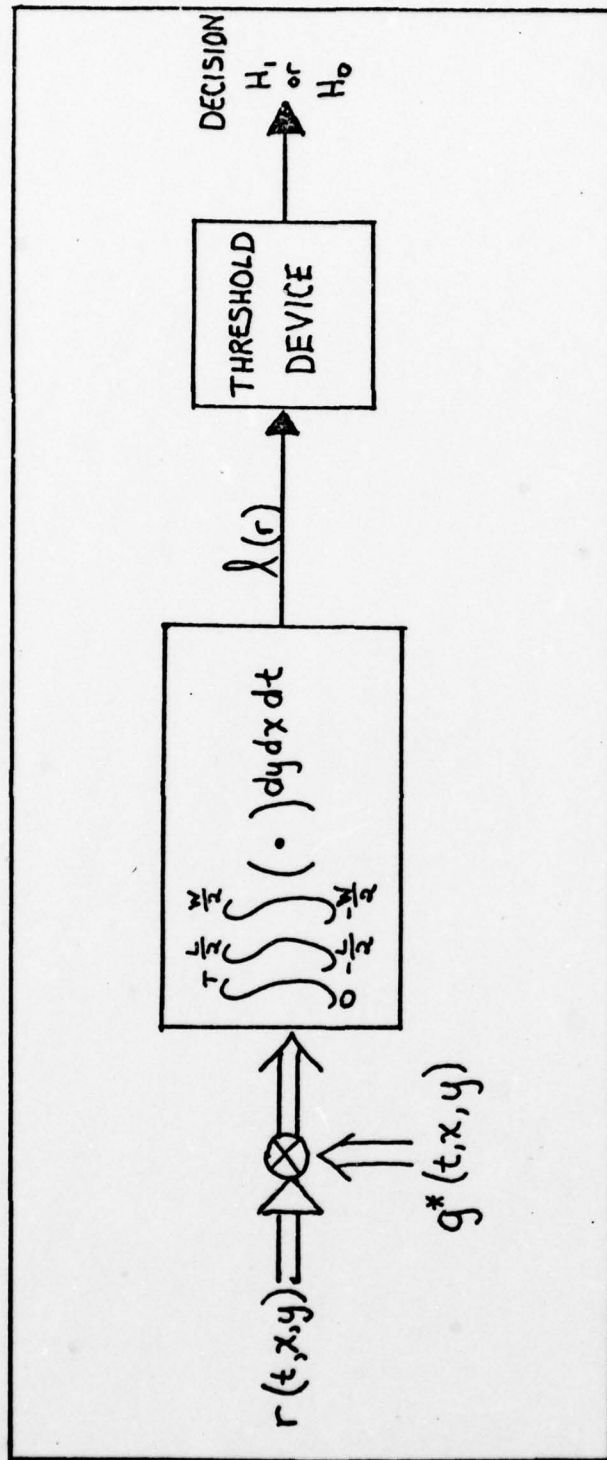


Figure 4. Complex optimum receiver configuration

1973:16). This measure is valuable for evaluating receiver performance when the signals are deterministic.

B. Optimum Array

In general to determine the sufficient statistic for the optimum array detector it is necessary to solve Eq (33) and then substitute the resulting Fredholm resolvent in Eq (32). However, for a continuous wave CW signal and CW jammers there is no time dependence in either of these signals. In other words, the desired signal has constant amplitude as does each of the jammers. Constant amplitudes for the jammers implies that the jammers temporal correlation function $R_J(\tau)$ is a constant, J_0 . Using the CW signals in Eq (33) yields:

$$s(\bar{r}) = N_0 g(t, \bar{r}) + J_0 \int_0^T \int_{-\frac{L}{2}}^{\frac{L}{2}} \int_{-\frac{W}{2}}^{\frac{W}{2}} g(t', \bar{r}') R_S(\bar{r} - \bar{r}') dt' d\bar{r}' \quad (37)$$

where $R_N(\tau, \bar{r} - \bar{r}')$ was replaced by $[N_0 \delta(\tau) \delta(\bar{r} - \bar{r}') + J_0 R_S(\bar{r} - \bar{r}')]$. Since there is no time dependence in $R_S(\bar{r} - \bar{r}')$, the time integration is performed first to give:

$$s(\bar{r}) = N_0 g(t, \bar{r}) + J_0 \int_{-\frac{L}{2}}^{\frac{L}{2}} \int_{-\frac{W}{2}}^{\frac{W}{2}} \bar{g}(\bar{r}') R_S(\bar{r} - \bar{r}') d\bar{r}' \quad (38)$$

where

$$\bar{g}(\bar{r}') = \int_0^T g(t', \bar{r}') dt' \quad (39)$$

There is no time dependence in the left hand side of Eq (38) thus there can be no time dependence on the right hand side of Eq (38). The only way to realize the equality is for:

$$g(t, \bar{r}) = g(\bar{r}) \quad (40)$$

which then means

$$\bar{g}(\bar{r}') = Tg(\bar{r}') \quad (41)$$

Thus the Fredholm resolvent $g(t, \bar{r})$ has been shown to be time independent for CW signals and CW jammers. Eq (37) can now be rewritten using this fact to give:

$$s(\bar{r}) = N_o g(\bar{r}) + TJ_o \int_{-L/2}^{L/2} \int_{-W/2}^{W/2} g(\bar{r}') R_s(\bar{r} - \bar{r}') d\bar{r}' \quad (42)$$

The solution of Eq (41) for $g(\bar{r})$ when substituted into Eq (32) yields the processor shown in Fig. 5.

In general the kernel, $R_s(\bar{r} - \bar{r}')$, has an infinite number of eigenvalues and eigenfunctions and yields the following solution for $g(\bar{r})$ (Van Trees, 1968:316):

$$g(\bar{r}) = TJ_o \sum_{i=1}^{\infty} \frac{s_i}{\beta_i + N_o} \zeta_i(\bar{r}) \quad (43)$$

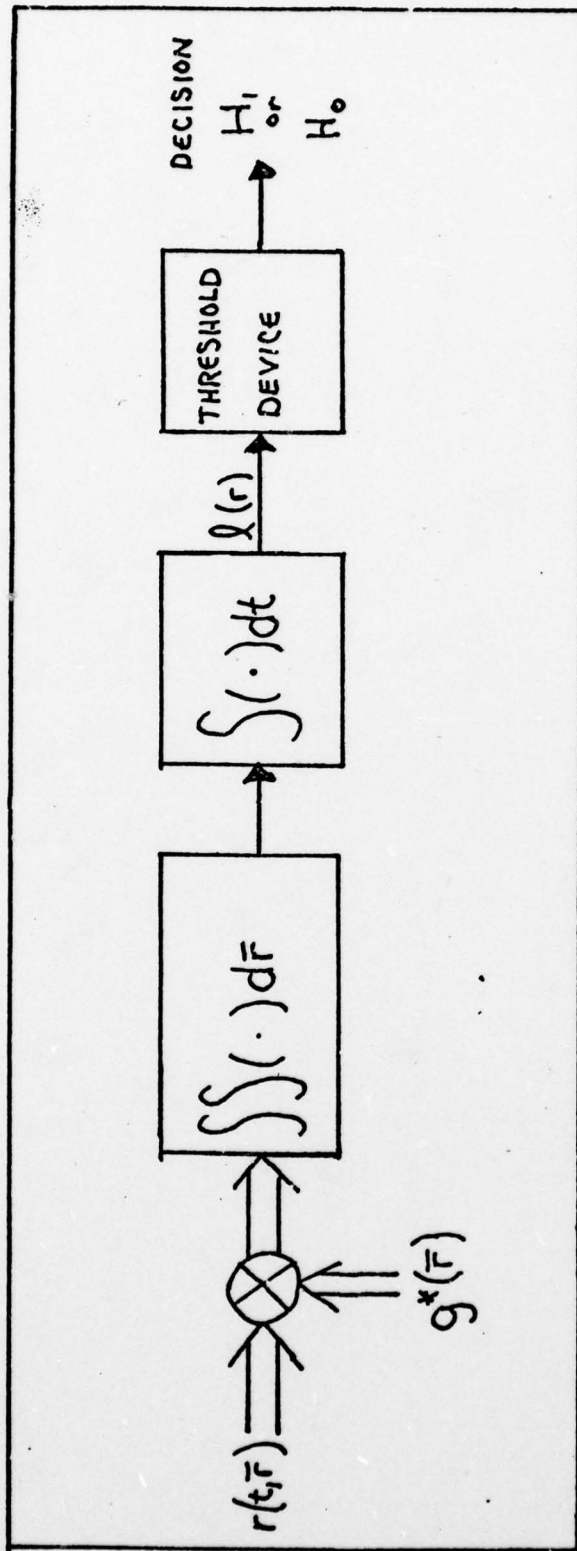


Figure 5. Optimum processor for CW signals and CW jammers

where the β_i are the eigenvalues and the $\zeta(\bar{r})$ are the eigenfunctions of $R_s(\bar{r}-\bar{r}')$. The s_i are given by:

$$s_i = \int_{-L/2}^{L/2} \int_{-W/2}^{W/2} s(\bar{r}) \zeta_i^*(\bar{r}) d\bar{r} \quad (44)$$

The use of an infinite number of eigenvalues does not represent a viable scenario for a jamming environment. To get a viable situation consider that $R_s(\bar{r}-\bar{r}')$ is a separable kernel and as such has the following solution for $g(\bar{r})$ (Van Trees, 1968:323):

$$\bar{g}(\bar{r}) = \frac{1}{N_o} \left[s(\bar{r}) - T J_o \sum_{i=1}^N \frac{s_i \beta_i}{\beta_i + N_o} \zeta_i(\bar{r}) \right] \quad (45)$$

For the case of N nearly orthogonal jammers, it has been demonstrated previously in Chapter II that for plane wave jammers the spatial eigenfunctions and spatial eigenvalues can be obtained by inspection from the spatial autocorrelation of the jammers. Thus using these eigenvalues and eigenfunctions in Eq (45) the spatial Fredholm resolvent for CW plane wave jammers is:

$$g(\bar{r}) = \frac{1}{N_o} \left[s(\bar{r}) - T J_o \sum_{i=1}^N \frac{s_i \alpha_i}{\alpha_i + N_o} T_i(\bar{r}) \right] \quad (46)$$

where $T(\bar{r})$ is as defined in Eq (29). Substituting this definition into Eq (45) yields:

$$g(\bar{r}) = \frac{1}{N_o} \left[s(\bar{r}) - J_o^T \sum_{i=1}^N \frac{s_i \alpha_i}{\alpha_i + N_o} \frac{\phi_i(\bar{r})}{\sqrt{LW}} \right] \quad (47)$$

where the $\phi_1(\bar{r})$ are as defined in Eq (18).

Once the Fredholm resolvent is known, the sufficient statistic and the performance can be determined for the optimum processor. In general, Eq (36) can be reduced to a simpler form for the binary hypothesis problem since the noise is zero mean. The substitution of Eq (32) in Eq (36) yields:

$$d_o^2 = \frac{\left[\begin{array}{c} T \quad L/2 \quad W/2 \\ \int \int \int s(t, \bar{r}) g^*(t, \bar{r}) dt d\bar{r} \\ 0 \quad -\frac{L}{2} \quad -\frac{W}{2} \end{array} \right]^2}{E \left[\begin{array}{c} T \quad L/2 \quad W/2 \\ \int \int \int n(t, \bar{r}) g^*(t, \bar{r}) dt d\bar{r} \quad \int \int \int n^*(t', \bar{r}') g(t', \bar{r}') dt' d\bar{r}' \\ 0 \quad -\frac{L}{2} \quad -\frac{W}{2} \end{array} \right]} \quad (48)$$

which becomes

$$d_o^2 = \frac{\left[\begin{array}{c} T \quad L/2 \quad W/2 \\ \int \int \int s(t, \bar{r}) g^*(t, \bar{r}) dt d\bar{r} \\ 0 \quad -\frac{L}{2} \quad -\frac{W}{2} \end{array} \right]^2}{\int \int \int \int \int \int R_N(\tau, \bar{r} - \bar{r}') g^*(t, \bar{r}) g(t', \bar{r}') dt dt' d\bar{r} d\bar{r}'} \quad (49)$$

Using Eq (33) in Eq (49) yields

$$d_o^2 = \frac{\int \int \int s(t, \bar{r}) g^*(t, \bar{r}) dt d\bar{r}}{\int \int \int \int \int \int R_N(\tau, \bar{r} - \bar{r}') g^*(t, \bar{r}) g(t', \bar{r}') dt dt' d\bar{r} d\bar{r}'} \quad (50)$$

which is the general result for the performance measure of the optimum detector. For the CW plane wave case, where the

Fredholm resolvent is given by Eq (45) and Eq (31) is true for the CW signal, then the performance measure is:

$$d_o^2 = \frac{E}{N_o} - \frac{J_o^T}{N_o} \sum_{i=1}^N \frac{s_i^2 \beta_i}{N_o + \beta_i} \quad (51)$$

The next step is to find the performance measure of the conventional detector when it is operating in the same jamming environment.

C. Conventional Array Detector

The conventional array detector is one which is optimized for performance in the presence of white noise only (Van Trees, 1971:152). The development is along the same line of thought as for the optimum array detector except the noise does not have a colored component (which is likened to saying that the amplitude of the CW jammer, J_o , is zero). With this in mind, Eq (37) becomes:

$$s(\bar{r}) = N_o g(\bar{r}) \quad (52)$$

Thus the Fredholm resolvent for the conventional array detector is quite obviously

$$g(\bar{r}) = \frac{1}{N_o} s(\bar{r}) \quad (53)$$

The representation of the conventional detector is commonly called a correlation receiver. The correlation receiver is also termed a beamformer in the case of an array detector (Gallop, 1971:57).

Since the beamformer is optimized for white noise only, it is interesting to note its performance in the presence of the spatially correlated noise used to optimize the optimum detector. This noise is given by:

$$R_N(\bar{r}-\bar{r}') = N_o \delta(\bar{r}-\bar{r}') + J_o R_s(\bar{r}-\bar{r}') \quad (54)$$

Substitution of Eq (54) into Eq (49) yields:

$$d_c^2 = \frac{\left[\int_0^T \int_{-L/2}^{L/2} \int_{-W/2}^{W/2} s(\bar{r}) g^*(\bar{r}) d\bar{r} dt \right]^2}{\int_0^T \int_0^T \int_{-L/2}^{L/2} \int_{-W/2}^{W/2} N_o g(\bar{r}) g^*(\bar{r}) dt' dt d\bar{r} + \int_0^T \int_0^T \int_{-L/2}^{L/2} \int_{-W/2}^{W/2} \int_{-L/2}^{L/2} \int_{-W/2}^{W/2} g(\bar{r}) g^*(\bar{r}') J_o R_s(\bar{r}-\bar{r}') dt d\bar{r} dt' d\bar{r}'}$$
(55)

Using Eq (52) in Eq (55) results in the following expression:

$$d_c^2 = \frac{\left[\int_0^T \int_{-L/2}^{L/2} \int_{-W/2}^{W/2} s(\bar{r}) g^*(\bar{r}) d\bar{r} dt \right]^2}{\int_0^T \int_0^T \int_{-L/2}^{L/2} \int_{-W/2}^{W/2} s(\bar{r}) g^*(\bar{r}) d\bar{r} dt dt' + \int_0^T \int_0^T \int_{-L/2}^{L/2} \int_{-L/2}^{L/2} \int_{-W/2}^{W/2} \int_{-W/2}^{W/2} g(\bar{r}) g^*(\bar{r}') J_o R_s(\bar{r}-\bar{r}') dt dt' d\bar{r} d\bar{r}'}$$
(56)

Substituting for $R_s(\bar{r}-\bar{r}')$ (Eq (24)) and having the signal again satisfy Eq (31), as done for the optimum detector, then the following performance measure for the conventional detector is obtained:

$$d_c^2 = \frac{E^2}{EN_o + J_o^T \sum_{i=1}^N \beta_{s_i}^2} \quad (57)$$

Having the expression in Eq (57) permits comparison of the conventional array detector with the optimum array detector for various jamming scenarios.

This chapter has developed the tools necessary to evaluate the performance of both the optimum and conventional array detectors. The next chapter uses these tools to develop an insight into the performance improvement afforded by the optimum array processor over the conventional processor.

IV. Performance Improvement

This chapter will discuss the performance improvement that the optimum array detector provides over the conventional beamformer in a jamming environment composed of CW plane wave signals. First, the method of comparing the two detectors will be discussed. Next three jamming scenarios will cover two cases of multiple jammers and a degenerate case of a single jammer requiring only one spatial dimension for processing. The two multiple jammer scenarios are first the case of N nearly orthogonal jammers and second the case of N jammers which cannot be individually resolved by the array. The performance comparisons made for each scenario will demonstrate the superior performance of the optimum array detector over the conventional beamformer.

A. Performance Measure

In order to compare the performances of the optimum and conventional detectors it is necessary to develop a measure of the improvement. One such measure is to simply compare the output signal to noise ratios for each of the detectors. This comparison is denoted μ and is defined as

$$\mu \triangleq \frac{d_o^2}{d_c^2} \quad (58)$$

where d_c^2 is the output signal to noise ratio (performance

measure) of the optimum array detector and d_c^2 is the output signal to noise ratio of the conventional detector. Clearly the regimes of μ which are of greatest interest when μ is much greater than one and when μ is approximately equal to one. The first regime (μ much greater than one) indicates that the optimum array detector performs much better than the conventional detector. The second regime (μ approximately equal to one) indicates that both the optimum and conventional detectors perform about the same.

Recalling Eqs (51) and (57), which are the general expressions for the performance measures of the optimum and conventional detectors in the presence of CW plane wave jammers, the ratio μ has the form:

$$\mu = \frac{\frac{E}{N_0} - \frac{J_0^T}{N_0} \sum_{i=1}^N \frac{s_1^2 \beta_1}{N_0 + \beta_1}}{\frac{E^2}{EN_0 + J_0^T \sum_{i=1}^N \beta_1 s_1^2}} \quad (59)$$

which can be rewritten

$$\mu = \left[1 - \frac{J_0}{N_0} \sum_{i=1}^N \frac{\beta_1 s_1'^2}{N_0 + \beta_1} \right] \left[1 + \frac{J_0}{N_0} \sum_{i=1}^N \beta_1 s_1'^2 \right] \quad (60)$$

where

$$s_1'^2 = \frac{s_1^2}{\int_{-L/2}^{L/2} \int_{-W/2}^{W/2} s(x,y) s^*(x,y) dx dy} \quad (61)$$

and

$$E = \begin{bmatrix} L/2 & W/2 \\ -L/2 & -W/2 \end{bmatrix} \int \int s(x,y) s^*(x,y) \quad T \quad (62)$$

This normalizes the signal energy and leads to an expression which is more easily interpreted. The expression in Eq (60) is valid for comparing the performance of the optimum and conventional detectors in an environment of CW jammers so long as the colored noise component results in a separable kernel. The discussions are all special cases of Eq (60).

B. N Nearly Orthogonal Jammers

The scenario involving N nearly orthogonal CW plane wave jammers requires that the criterion established in Eq (27) be met. With this criterion met, Eq (60) becomes:

$$\mu = 1 + (LW)^2 J^2 \left\{ \frac{\sum_{i=1}^N \sum_{j=1}^N \alpha_i \alpha_j}{(LW \alpha_i + N_o) N_o} \left[\sum_{i=1}^N s_i'^2 \left(1 - \sum_{j=1}^N s_j'^2 \right) \right] \right\} \quad (63)$$

where the β_i are $LW\alpha_i$ (recall α_i from Eq (29) and the s_i' are given by:

$$s_i' = \begin{bmatrix} \frac{\sin(v_{sx} - v_{nxi}) \frac{L}{2}}{\frac{L}{2}(v_{sx} - v_{nxi})} \\ \frac{\sin(v_{sy} - v_{nyi}) \frac{W}{2}}{\frac{W}{2}(v_{sy} - v_{nyi})} \end{bmatrix} \quad (64)$$

where v_{sx} , v_{sy} , v_{nxi} , and v_{nyi} are the spatial frequencies of the signal and jammer and are given by:

$$v_{sx} = \frac{\cos\theta}{\lambda_s} \quad (65a)$$

$$v_{sy} = \frac{\cos\phi}{\lambda_s} \quad (65b)$$

$$v_{nxi} = \frac{\cos\theta_1}{\lambda_n} \quad (65c)$$

$$v_{nyi} = \frac{\cos\phi_1}{\lambda_n} \quad (65d)$$

and the θ_s , θ_{ni} , ϕ_s and ϕ_{ni} are the incident angles relative to the array's x and y coordinate (recall Fig. 3) for the signal and jammers. The eigenfunctions used to compute the s'_1 are given by Eq (29) as previously discussed. After applying the assumption that the signal and jammers are at the same wavelength, λ_s , and recalling the definition of $\text{sinc}(x)$ in Eq (28), Eq (64) becomes

$$s'_1 = \text{sinc} \left[\frac{L\pi}{\lambda_s} (\cos\theta_s - \cos\theta_{ni}) \right] \text{sinc} \left[\frac{W\pi}{\lambda_s} (\cos\phi_s - \cos\phi_{ni}) \right] \quad (66)$$

Thus the significant aspect of Eq (63) with regard to the performance improvement is the value of the $s'_1{}^2$. The double

sum coefficient of the $s_i'^2$ in Eq (63) is always a positive number and serves to weight the terms involving the $s_i'^2$. Several observations can be made relative to the performance improvement.

First, when all of the $s_i'^2$ are zero, then the performance indicator, μ is unity. This situation occurs when the signal is nearly orthogonal to all of the jammers. In this case, the conventional detector can detect the signal as well as the optimum detector since the effect of the jammers has been neutralized by the mutual orthogonality of the signal and jammers.

Second, μ is also unity if the $s_i'^2$ all sum to one. This situation occurs if the signal is perfectly aligned with one of the jammers. Then, in this case, both the optimum and conventional detectors perform equally poorly.

The above discussion addressed the cases of equal performance for the optimum and conventional detectors. These cases are interesting, but the case of greatest interest is that in which the optimum detector is clearly superior to the conventional detector (μ is much greater than unity). To look at this case, consider first, that due to the mutual orthogonality, the signal will project only on those jammers who fall within the resolution range of the array when it's main beam is directed at the signal. All other jammers will have no effect upon the signal.

For the case when there are two jammers close enough for the signal to project on each of them, the Eq (63) becomes:

$$\mu = 1 + \frac{(LW)^2 J_o^2}{N_o} \left\{ \left[\frac{\alpha_1}{(LW\alpha_1 + N_o)} + \frac{\alpha_2}{(LW\alpha_2 + N_o)} \right] (\alpha_1 + \alpha_2) \right. \\ \left. (s_1'^2 + s_2'^2) \left[1 - (s_1'^2 + s_2'^2) \right] \right\} \quad (67)$$

Eq (67) can be simplified greatly if the following relationships are assumed:

$$\alpha_1 = \alpha_2 \quad (68a)$$

and

$$s_1'^2 = s_2'^2 \quad (68b)$$

Eq (68a) implies the two jammers are of equal strength. Eq (68b) implies that the signal projects equally onto each jammer. Stated another way, the signal is angularly equidistant from each jammer in either the x or y dimension.

Then Eq (67) becomes:

$$\mu = 1 + \frac{(LW)^2 J_o^2 16}{N_o} \left\{ \frac{\alpha_1^2}{(LW\alpha_1 + N_o)} \left[s_1'^2 \left(\frac{1}{2} - s_1'^2 \right) \right] \right\} \quad (69)$$

or by letting γ be given by

$$\gamma = \frac{16(Lw)^2 J_o^2}{N_o} \left[\frac{\alpha_1^2}{(LW\alpha_1 + N_o)} \right] \quad (70)$$

then Eq (69) becomes

$$\mu = 1 + \gamma [s_1'^2 (\frac{1}{2} - s_1'^2)] \quad (71)$$

where $s_1'^2$ is given by

$$s_1'^2 = \text{sinc}^2 \left[\frac{L\pi}{\lambda_s} (\cos\theta_s - \cos\theta_{ni}) \right] \text{sinc}^2 \left[\frac{W}{\lambda_s} (\cos\phi_s - \cos\phi_{ni}) \right] \quad (72)$$

From Eq (72) and the assumptions made in Eq (68b), it is clear that $s_1'^2$ is bounded by zero and one-half. Fig. 6 plots Eq (71) as a function of $s_1'^2$. From Fig. 6, the maximum value of μ occurs when $s_1'^2$ equals one-fourth and is given by

$$\mu_{\max} = 1 + .0625\gamma \quad (73)$$

This situation represents the fact that the signal projects twenty five percent of its power in the direction of each of the two jammers. For μ to be much greater than unity, it is necessary for the following condition to be true:

$$\gamma s_1'^2 (\frac{1}{2} - s_1'^2) \gg 1 \quad (74)$$

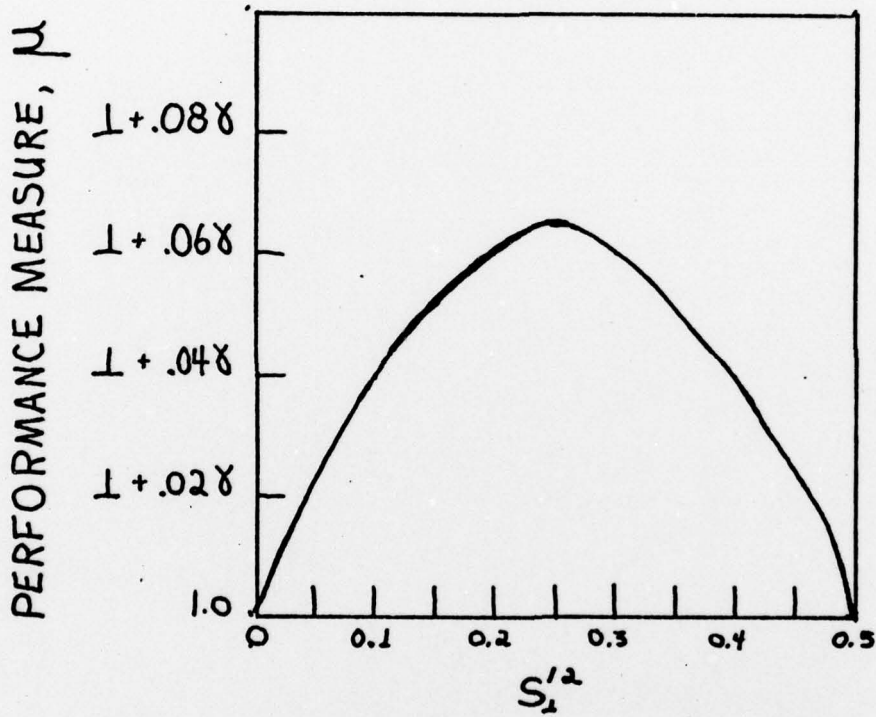


Figure 6. Performance measure, μ , versus $s_1^{1/2}$ for two jammers.

Recalling Eq (69), the condition described in Eq (74) occurs when the following situation exists:

$$\frac{N_o}{4J_o\alpha_1LW} \ll s_1'^2 \ll 1 \quad (75)$$

which says that twenty five percent of the thermal noise (N_o) to interference power ($J_o\alpha_1LW$) ratio is much less than the signal power in the interference direction. Thus by knowing the thermal noise of the array, the array size, the interference power and the location of the jammers in both spatial dimensions, the signal location can be positioned to achieve the criterion established in Eq (75). Alternately, knowledge and ability to change any of the parameters permits the optimum detector to be peaked for maximum performance improvement for a given situation.

As an example, consider letting the ratio of the interference power to the thermal noise be 30dB and the value for $s_1'^2$ be 0.1, then the criterion in Eq (75) are satisfied and substitution into Eq (69) indicates that the performance improvement of the optimum detector is on the order of 68dB. Computing d_o^2 using Eq (51) and d_c^2 using Eq (57) for the same condition yields:

$$d_o^2 = 101\text{dB} \quad (76a)$$

$$d_c^2 = 33\text{dB} \quad (76b)$$

These results are for a normalized signal energy and indicate that the optimum detector is clearly better than the beam-former.

Before concluding the mutually orthogonal jammer scenario, an interesting degenerate case is the one for only a single jammer present. For the single jammer, Eq (63) becomes:

$$\mu = 1 + \left[\frac{(LW)^2 \alpha^2 J_o^2}{(LW\alpha + N_o) N_o} \right] s'^2 [1 - s'^2] \quad (77)$$

where s'^2 is given by Eq (72) when the subscripts are deleted.

For the single jammer case, s'^2 is bounded by zero and one.

Fig. 7 plots the following function versus s'^2 :

$$\mu = 1 + \gamma' s'^2 (1 - s'^2) \quad (78)$$

where γ' is the constant coefficient in Eq (77).

From Fig. 7, the maximum value occurs when s'^2 equals one-half and is given by:

$$\mu_{\max} = 1 + .25\gamma' \quad (79)$$

This situation represents the fact that the signal projects fifty percent of its power in the direction of the jammer (Pasupathy, 1978:161). For μ to be much greater than unity it is necessary for the following criterion to be true:

$$\gamma' s'^2(1-s'^2) \gg 1 \quad (80)$$

This condition occurs when

$$\frac{N_o}{J_o \alpha L W} \ll s'^2 \ll 1 \quad (81)$$

which says the ratio of thermal noise to interference power is much less than the signal power in the interference direction. Using the same example as used previously for the two nearly orthogonal jammers, the performance improvement of the optimum detector over the beamformer is now 60dB. Again the example was done for a unit energy signal.

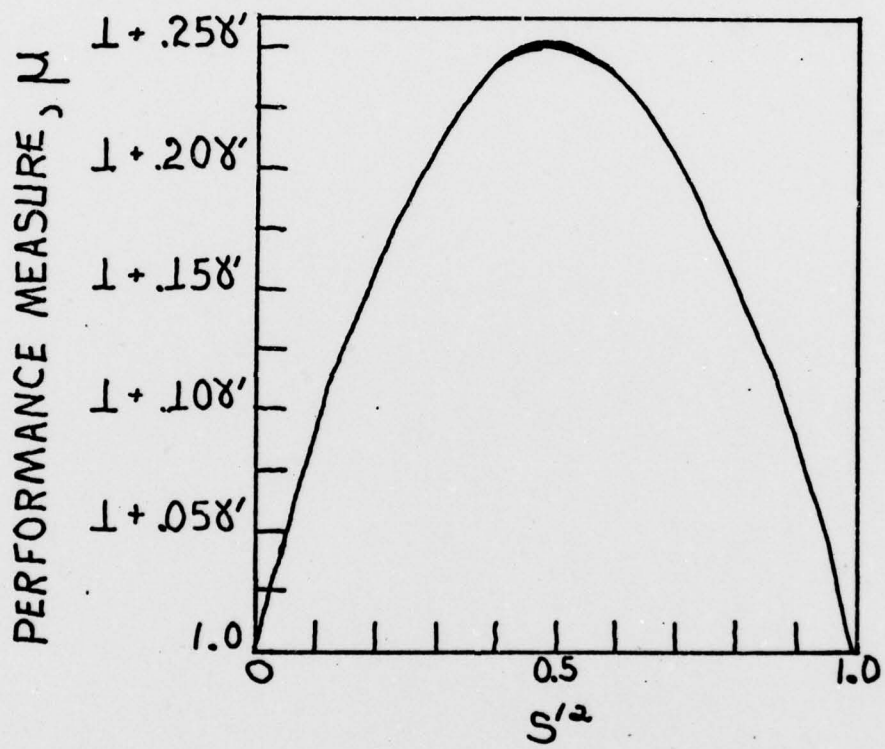


Figure 7. Performance measure, μ , versus s'^2 for one jammer

C. N Non-Resolvable Jammers

The next jamming scenario of interest is the scenario in which the array cannot resolve the individual jammers due to insufficient angular separation among the jammers. This case corresponds to having a single spatially band-limited jammer with N significant eigenvalues. If the N jammers are all of equal power then the eigenvalues can be considered to be approximately equal. Thus the expression for μ given by Eq (60) becomes:

$$\mu = 1 + \frac{\eta^2 J_c^2}{(\eta + N_o) N_o} \left[\sum_{i=1}^N s_i'^2 (1 - \sum_{i=1}^N s_i'^2) \right] \quad (82)$$

where η is the significant eigenvalue and the s_i' are as previously defined in Eq (61) and Eq (44). The notable difference between this case and the case of N nearly orthogonal jammers is the determination of the eigenfunctions. For the orthogonal jammers, the eigenfunctions were the weighted exponential propagation functions of each jammer. For the band-limited case, the eigenfunctions need to be computed. This determination of the eigenfunctions must be done for specific examples and cannot be done in general. However, by interpreting the summation of the $s_i'^2$ as the signal power in the interference beamwidth of the array (Pasupathy, 1978:161), it is possible to develop an intuition about the performance improvement of the optimum detector versus the conventional detector. By redefining the summation of the $s_i'^2$, Eq (82) becomes

$$\mu = 1 + \frac{\eta^2 J_o^2}{(\eta + N_o) N_o} \sigma^2 (1 - \sigma^2) \quad (83)$$

where

$$\sigma^2 = \frac{N}{\sum_{i=1}^N s_i'^2} \quad (84)$$

Comparing Eq (83) with Eq (77), it is obvious that the two equations are of the same form, differing only in the constant coefficient. Thus, the same analysis is valid as was performed for the single jammer in the previous section with some amplifying observations regarding the physical interpretations.

When σ^2 is equal to one-half, μ achieves its maximum value and is given by:

$$\mu_{\max} \approx .25 \frac{\eta J_o}{N_o} \quad (85)$$

when η is much greater than the thermal noise, N_o . To interpret Eq (85), it is necessary to look at d_o^2 and d_c^2 . These quantities are given by

$$d_o^2 \approx \frac{1}{N_o} \quad J_o \eta \gg N_o, \quad \sigma^2 = \frac{1}{2} \quad (86a)$$

and

$$d_c^2 \approx \frac{1}{N_o \left(\frac{\eta J_o}{2N_o} \right)} \quad J_o \eta \gg N_o, \quad \sigma^2 = \frac{1}{2} \quad (86b)$$

Evidently, d_o^2 is independent of η for the given situation but d_o^2 depends inversely on the relationship between ηJ_o and N_o . Thus the performance improvement indicated by μ_{\max} is primarily due to a degradation of the conventional detector performance rather than an increase in the performance of the optimum detector (Pasupathy, 1978:162). This was not the case for the orthogonal jammer scenario. In that scenario the performance improvement was tied to both the improvement afforded by the optimum detector and the degradation of the conventional detector.

To quantify this scenario in terms of performance improvement as previously done, consider letting ηJ_o be much greater than N_o , and the ratio $\frac{\eta J_o}{N_o}$ be equal to 30dB, then for a σ^2 equal to 0.1 the performance improvement is approximately 19.5dB when all of the assumptions and conditions are substituted into Eq (83). The fact that this scenario has N jammers is contained in the σ^2 and variations in the results due to a different number of jammers are attributed to variations in σ^2 .

D. Single Jammer, Single Spatial Dimension

The final jamming scenario is really a degenerate case of the single jammer scenario discussed for two spatial dimensions. This degenerate case is one in which it is necessary to look only at a single spatial dimension. The degenerate case comes about when either of the sinc functions in Eq (66) is unity. This means that the signal and jammer are aligned in one of the spatial dimensions. With this being the case, it

is necessary to look only at the single spatial dimension to determine the performance improvement. Thus for the one dimension case Eq (77) becomes:

$$\mu = 1 + \frac{L^2 \alpha^2 J_o^2}{(L\alpha + N_o) N_o} q^2 (1 - q^2) \quad (87)$$

where q^2 is given by:

$$q^2 = \text{sinc}^2 \left[\frac{L\pi}{\lambda_s} (\cos \theta_s - \cos \theta_n) \right] \quad (88)$$

Again the same interpretations as made for the two dimension single jammer case apply. Fig. 8 illustrates a specific example of the one dimension case. Given that α , N_o , λ_s , and L are all fixed for the example, it is easy to see the effect of different angular separations between the signal and the jammer. Thus, Fig. 8 indicates the improvement for different signal incident angles (θ_s) to the array of the optimum detector over the conventional detector. For example, given that the array could be easily reoriented so as to change the incident angle of the signal, then knowledge of the angular difference ($\Delta\theta$) between the signal and jammer would indicate which incident angle would provide the greatest performance improvement. Also from Fig. 8 the performance improvement for the example which has been used in all of the previous scenarios is given to be approximately 20dB.

This chapter has succeeded in developing a performance measure, μ , which was used to evaluate three jamming scenarios. The three jamming scenarios were evaluated with a common

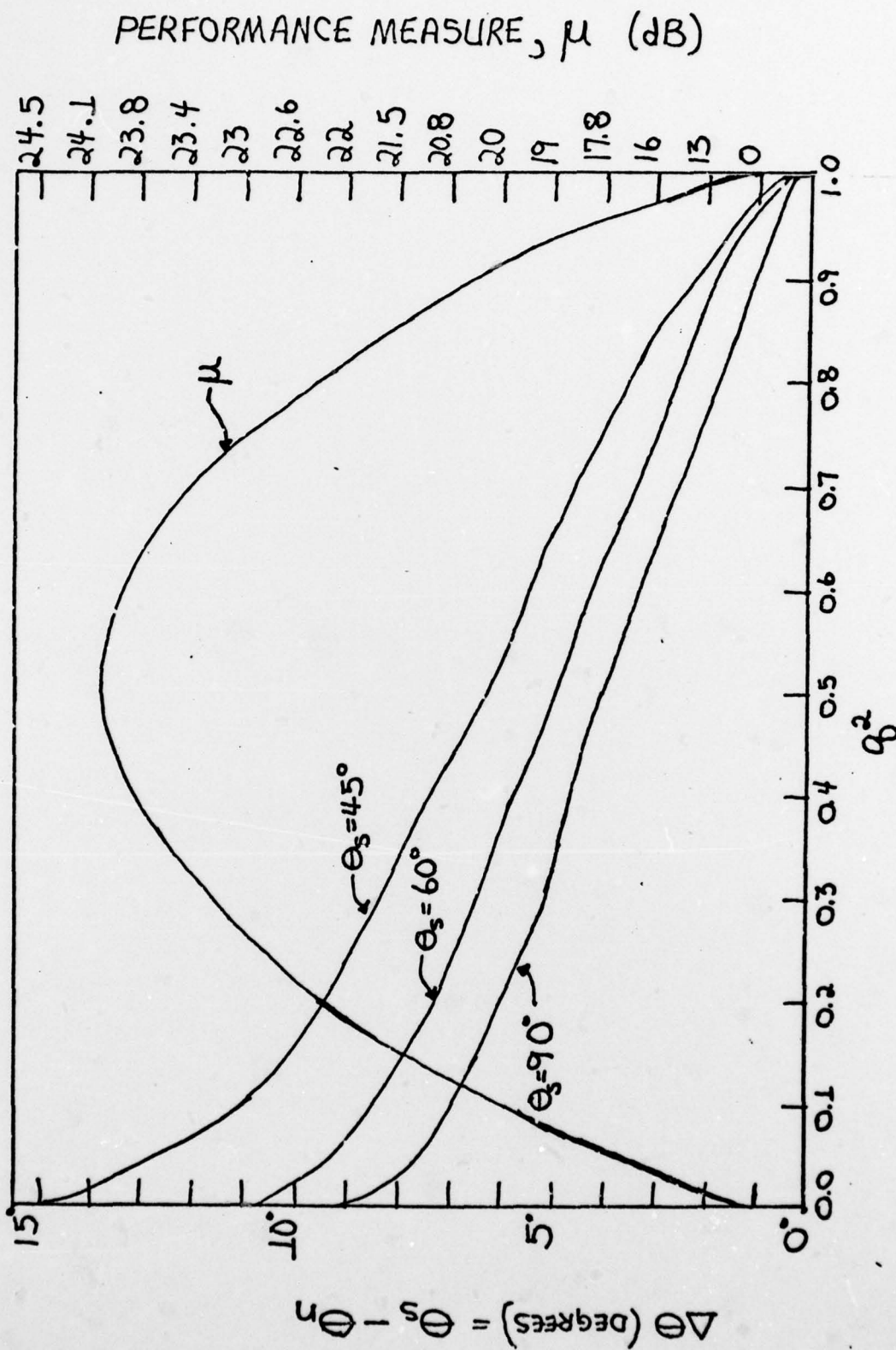


Figure 8. Angular difference ($\theta_s - \theta_n$) versus q^2 ; μ versus q^2 for $\lambda_n = \lambda_s = 0.5m$, $L = 1m$, $\frac{J_0 \alpha L}{N_0} = 30dB$.

example and it was shown that the optimum array detector is significantly better than the beamformer. Additionally physical interpretations were made to enhance the information provided by the performance comparisons. The final conclusions of this thesis and recommendations for additional research are addressed in the next chapter.

V. Conclusions and Recommendations

A. Conclusions

The preceding discussion has developed three areas. First, the representation of several jamming scenarios as a colored noise component in the noise term of the binary hypothesis detection problem. Second, a measure of performance improvement, μ , was developed by comparing the output signal to noise ratios of the optimum and conventional array detectors. Analysis of the performance improvement was presented for the jamming scenarios of interest based on total knowledge of the desired signal and the jamming signals. This analysis developed relationships which identified the parameters which the system designer could address to achieve maximum improvement from the optimum array detector. Finally, an example was presented for each scenario which showed that the optimum array detector was significantly better than the beamformer.

Several of the points previously made need to be reiterated. First, for single jammers, the maximum performance improvement is achieved by the optimum detector when fifty percent of the signal power is projected in the jammer's direction. This is also valid for multiple jammer situations when the signal is nearly orthogonal to all but one of the jammers. Secondly, for single jammers and N nearly orthogonal jammers the thermal noise/interference power ratio must be much less than the signal power in the jamming direction to achieve significant

performance improvements. In the case of the non-resolvable jammers it was seen that significant performance improvement was largely due to degradation of the conventional detector rather than the improved performance of the optimum detector.

These observations bring out two points which are applicable to the array problem. First, the signal power and the projection of the signal power in the interference (jamming) direction significantly affect the performance of the detectors. Secondly, the thermal noise, in the case of the non-resolvable jammers particularly, is a significantly contributing factor in the performance of the detectors.

It is recognized that the criterion which allows the single spatial dimension degeneration is probabilistically very unrealizable. None the less, the single spatial dimension provides the ability to get a "back of the envelope" approximation which, when compared to the two spatial dimension results, provided the engineer with an insight into the problem without a great deal of effort.

Finally, a single example was exercised for each scenario. In this example the ratio of jammer interference power to thermal noise was equal to 30dB and the parameter related to the projection of the signal onto the jammer was equal to 0.1. The resulting performance improvements were 68dB, 60dB, 19.5dB, and 20dB for the two orthogonal jammers, single jammer (two spatial dimensions), spatially bandlimited jammer, and the single jammer, (single spatial dimension) respectively. The variations

in the performance improvement are related to the complexity of the individual jamming scenario. However, all of the scenarios indicate that the optimum array detector is clearly better than the beamformer.

B. Recommendations

The previous work is based on full knowledge of the signal and the jammers, particularly with regard to amplitude and direction. This fact suggests that future research should extend the assessment of performance improvement by relaxing the assumptions which were made in this study. Specifically, addressing the performance improvement for time varying amplitudes for both the desired signal and jammers and the inclusion of temporally dependent signals would be the next logical extension of this research. Succeeding extensions of the effort would include examination of signals with random amplitude and random phase, and a relaxation of the directional knowledge of the signal's location. Completion of these research tasks would provide a relatively complete picture of the performance improvement that an optimum array detector can provide.

Bibliography

- Adams, S.L., The Theory of Signal Detectability: Extension to Optimum Arrays. Adaptive Signal Detection Laboratory TR-9. Durham, North Carolina: Duke University, July, 1973 (AD 780 241).
- Adams, S.L., and L.W. Nolte, "Bayes Optimum Array Detection of Targets of Known Location," Journal of the Acoustical Society of America, 58:656-669 (September 1975).
- Davenport, Wilbur B., and William Root. An Introduction to the Theory of Random Signals and Noise. New York: McGraw-Hill Book Company, Inc., 1958.
- Dudgeon, D.E. "Fundamentals of Digital Array Processing," Proceedings of the IEEE, 65: 898-904 (June 1977).
- Gagliardi, R.M., and Sherrman Karp. Optical Communications. New York: John Wiley and Sons, 1976.
- Gallop, M.A., Jr. Adaptive Optimum Array Detectors. Adaptive signal Detection Laboratory TR-7. Durham, North Carolina: Duke University, May 1971.
- Gallop, M.A., Jr., and L.W. Nolte, "Bayesian Detection of Targets of Unknown Location," IEEE Transactions on Aerospace and Electronic Systems, AES-10: 429-435 (July 1974).
- Hodgkiss, W.S.. and L.W. Nolte, "Optimal Array Processor Performance Trade-offs Under Directional Uncertainty," IEEE Transactions on Aerospace and Electronic Systems, AES-12: 605-615 (September 1976).
- Melen, Roger and Dennis Buss, editors. Changed-Coupled Devices: Technology and Applications. New York: IEEE Press, 1977.
- Papoulis, Athanasios. Probability, Random Variables, and Stochastic Processes. New York: McGraw-Hill Book Company, Inc., 1965.
- Pasupathy, Subbarayan. "Optimum Spatial Processing of Passive Sonar Signals," IEEE Transactions on Aerospace and Electronic Systems, AES-14: 158-164 (January 1978).

Van Trees, H.L. Detection, Estimation, and Modulation Theory, Part I. New York: John Wiley and Sons, 1968.

Detection, Estimation and Modulation Theory, Part III.
New York: John Wiley and Sons, 1971.

Vita

Captain Ronnie Ellis Lesher was born at MacDill AFB, Florida on 24 June 1947. He was graduated from H. B. Plant High School, Tampa, Florida, in June of 1965. In June 1969, Captain Lesher was graduated from Duke University with a Bachelor of Science in Physics. Subsequently, he received the Master of Science in Systems Management degree from the University of Southern California in June 1973.

Captain Lesher was commissioned through the ROTC program at Duke University in June 1969. Upon completion of the Communications-Electronics officers Course at Keesler AFB, Mississippi in March 1970, Captain Lesher was assigned to Headquarters Pacific Communications Area (AFCS) at Hickam AFB, Hawaii where he served as a communications duty officer in the Pacific Air Forces (PACAF) Command Post. He also served as the Chief, Systems Operations Branch, and Chief, NAVAIDS Communications Management Office while assigned to Pacific Communications Area Headquarters. He was then assigned to Headquarters Tactical Communications Area (AFCS), Langley AFB, Virginia and served as a Communications Concepts, Requirements, and Plans officer for future tactical communications equipment. Captain Lesher has completed Squadron Officers School and the USAF Air Command and Staff

College. In June 1976, Captain Lesher was assigned to the Air Force Institute of Technology, School of Engineering and completed the Post Graduate Engineering Science Program in June 1977.

Permanent Address: 4118 Palmira Street
Tampa, Florida 33609

UNCLASSIFIED

SECURITY CLASSIFICATION OF THIS PAGE (When Data Entered)

REPORT DOCUMENTATION PAGE		READ INSTRUCTIONS BEFORE COMPLETING FORM
1. REPORT NUMBER AFIT/GE/EE/78-33	2. GOVT ACCESSION NO.	3. RECIPIENT'S CATALOG NUMBER
4. TITLE (and Subtitle) PERFORMANCE IMPROVEMENT OF A CLASS OF ARRAY PROCESSORS IN A JAMMING ENVIRONMENT		5. TYPE OF REPORT & PERIOD COVERED MS Thesis
		6. PERFORMING ORG. REPORT NUMBER
7. AUTHOR(s) Ronnie E. Leshner Capt USAF		8. CONTRACT OR GRANT NUMBER(s)
9. PERFORMING ORGANIZATION NAME AND ADDRESS Air Force Institute of Technology (AFIT/EN) Wright-Patterson AFB OH 45433		10. PROGRAM ELEMENT, PROJECT, TASK AREA & WORK UNIT NUMBERS 63727F/2277
11. CONTROLLING OFFICE NAME AND ADDRESS Rome Air Development Center/DCID Griffiss AFB NY 13441		12. REPORT DATE December 1978 ✓
		13. NUMBER OF PAGES 61
14. MONITORING AGENCY NAME & ADDRESS (if different from Controlling Office)		15. SECURITY CLASS. (of this report) UNCLASSIFIED
		15a. DECLASSIFICATION/DOWNGRADING SCHEDULE
16. DISTRIBUTION STATEMENT (of this Report) Approved for public release; distribution unlimited		
17. DISTRIBUTION STATEMENT (of the abstract entered in Block 20, if different from Report)		
18. SUPPLEMENTARY NOTES Approved for public release; IAW AFR 190-17 J.P. HIPPS, Maj, USAF Director of Information 1-23-79		
19. KEY WORDS (Continue on reverse side if necessary and identify by block number) Optimum Signal Detection Signals Know Exactly Array Antenna Systems Jamming Environment Detection Performance Signal Representation Optimum Space-Time Processing Binary Hypothesis Receiver Structure Interfering Signals		
20. ABSTRACT (Continue on reverse side if necessary and identify by block number) The purpose of this research is to determine the fundamental performance improvement of an optimum array detector versus a conventional beamformer detector in a jamming environment. The fundamental performance improvement is based on total knowledge of both the desired signal and the jammers, and their respective locations in space. The jammers are modeled as a colored noise component in the binary hypothesis detection problem. Mathematical tractability is achieved by considering distributed measurements in space and		

DD FORM 1 JAN 73 1473

EDITION OF 1 NOV 65 IS OBSOLETE

UNCLASSIFIED

SECURITY CLASSIFICATION OF THIS PAGE (When Data Entered)

UNCLASSIFIED

SECURITY CLASSIFICATION OF THIS PAGE(When Data Entered)

time across the array. Conditions are identified which allow determination of the necessary eigenvalues and eigenfunctions by inspection of the propagation functions of plane wave jammers.)

Performance improvement is given for several jamming scenarios: two mutually orthogonal jammers, single jammer (two spatial dimensions), band limited jammer, and single jammer (one spatial dimension). The optimum detector performs respectively 68dB, 60dB, and 20dB better than the beamformer for the jamming scenarios addressed and similar parameters for each case. The maximum performance improvement for the two mutually orthogonal jammers occurs when twenty-five percent of the signal power projects in the direction of each jammer. → Maximum improvement for a single jammer occurs when fifty percent of the signal power projects in the direction of the jammer. Performance improvement in the presence of a spatially bandlimited jammer is due primarily to the degradation of the beamformer's performance. For the scenarios examined, the optimum detector provides significant performance improvement over the conventional beamformer detector.

SECURITY CLASSIFICATION OF THIS PAGE(When Data Entered)